We are IntechOpen, the world's leading publisher of Open Access books Built by scientists, for scientists

4,800
Open access books available

122,000
International authors and editors

135M
Downloads

Our authors are among the

154
Countries delivered to

TOP 1%
most cited scientists

12.2%
Contributors from top 500 universities

CLARIVATE ANALYTICS BOOK CITATION INDEX INDEXED

WEB OF SCIENCE™

Selection of our books indexed in the Book Citation Index in Web of Science™ Core Collection (BKCI)

Interested in publishing with us?
Contact book.department@intechopen.com

Numbers displayed above are based on latest data collected.
For more information visit www.intechopen.com

7

Modelling of Profile Evolution by Transport Transitions in Fusion Plasmas

Mikhail Tokar
Institute for Energy and Climate Research – Plasma Physics, Research Centre Jülich Germany

1. Introduction

In tokamaks, the most advanced types of fusion devices, electric currents, flowing both in external coils and inside the plasma itself, produce nested closed magnetic surfaces, see Fig. 1. This allows confining charged plasma components, electrons and deuterium-tritium fuel ions, throughout times exceeding by orders of magnitudes those which particles require to pass through the device if they would freely run away with their thermal velocities. Under conditions of ideal confinement charged particles would infinitely move along and rotate around magnetic field lines forming the surfaces. In reality, diverse transport processes lead to losses of particles and energy from the plasma. On the one hand, this hinders the attainment and maintenance of the plasma density and temperature on a required level and forces to develop sophisticated and expansive methods to feed and heat up the plasma components. On the other hand, if the fusion conditions are achieved the generated α-particles have to be transported out to avoid suffocation of the thermonuclear burning in a reactor. Therefore it is very important to investigate, understand, predict and control transport processes in fusion plasmas.

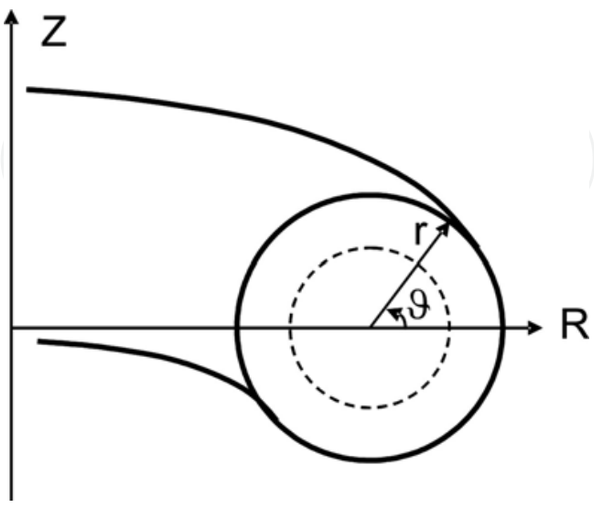

Fig. 1. Geometry of magnetic surface cross-sections in an axis-symmetrical tokamak device and normally used co-ordinate systems

1.1 Classical and neoclassical transport

Plasmas in magnetic fusion devices of the tokamak type are media with complex non-trivial characteristics of heat and mass transfer across magnetic surfaces. The most basic mechanism for transport phenomena is due to coulomb collisions of plasma components, electrons and ions. By such collisions the centres of Larmor circles, traced by particles, are displaced across the magnetic field B. In the case of light electrons this displacement is of their Larmor circle radius ρ_{Le}. Due to the momentum conservation the Larmor centres of ions are shifted at the same distance. Therefore the transport is automatically ambipolar and is determined by the electron characteristics only. The level of this so called classical diffusion can be estimated in a random step approximation, see, e.g., Ref. (Wesson, 2004):

$$D_{cl} \approx \rho_{Le}^2 \nu_e \tag{1}$$

with ν_e being the frequency of electron-ion collisions. Normally D_{cl} is very low, 10^{-3} m^2s^{-1}, and practically no experimental conditions have been found up to now in real fusion plasmas where the measured particle diffusivity would not significantly exceed this level. Mutual electron-electron and ion-ion collisions do not lead to net displacements and transfer of particles. But in the presence of temperature gradients they cause heat losses because particles of different temperatures are transferred across the magnetic surfaces in opposite directions. This heat transfer is by a factor of $\left(m_i/m_e\right)^{1/2}$ larger for ions than for electrons, where m_i and m_e are the corresponding particle masses, (Braginskii, 1963).

In a tokamak magnetic field lines are curved and, by moving along them, the charged particles are subjected to centrifugal forces. The plasma current produces the so called poloidal component of the magnetic field and therefore field lines have a spiral structure, displacing periodically from the outer to the inner side of the torus. Thus, when moving along them, charged particles go through regions of different field magnitude since the latter varies inversely proportional to the distance R from the torus axis analogously to the field from a current flowing along the axis. Because of their Larmor rotation the particles possess magnetic momentums and those fill a force in the direction of the field variation, i.e. in the same direction R as that of the centrifugal force. Both forces cause a particle drift motion perpendicular to the magnetic field and R, i.e. in the vertical direction Z, see Fig.1. In the upper half of the torus, $Z > 0$, this drift is directed outwards the magnetic surface and in the lower one, $Z < 0$, - towards the surface. Thus, after one turn in the poloidal direction ϑ the particle would not have a net radial displacement. This is not however the case if the particle motion is chaotically interrupted by coulomb collisions. As a result, the particle starts a new Larmor circle at a radial distance from the original surface exceeding the Larmor radius by q times where the safety factor q characterizes the pitch-angle of the field lines. This noticeably enhances, by an order of magnitude, the classical particle and energy transfer. Even more dramatic is the situation for particles moving too slowly along magnetic field: these are completely trapped in the local magnetic well at the outer low field side. They spent much longer time in the same half of the magnetic surface and deviate from it by a factor of $(R/r)^{1/2}$ stronger than passing particles freely flying along the torus. The poloidal projections of trajectories of such trapped particle look like "bananas". For the existence of "banana" trapped particles should not collide too often, i.e. the collision length λ_c has not to exceed $qR(R/r)^{3/2}$. In spite of the rareness of collisions, these lead to a transport contribution from trapped particles exceeding significantly, by a factor of $q^2(R/r)^{3/2}$, the classical one, see

Ref. (Galeev & Sagdeev, 1973). In an opposite case of very often collisions, where $\lambda_c << qR$, there are not at all particles passing a full poloidal circumference without collisions. In this, the so called Pfirsch-Schlüter, collision dominated regime the transport is enhanced with respect to the classical one by a factor of q^2. In the intermediate "plateau" range the transport coefficients are formally independent of the collision frequency. The transport contribution due to toroidal geometry described above is referred to as a "neoclassical" transport and is universally present in toroidal fusion devices. Fortunately, under high thermonuclear temperatures it causes only a small enough and, therefore, quite acceptable level of losses.

1.2 Anomalous transport

The sources of charged particles and energy inside the plasma result in sharp gradients of the temperature T and density n in the radial direction r across the magnetic surfaces. Thus, a vast reservoir of free energy is stored in the plasma core. This may be released by triggering of drift waves, perturbations of the plasma density and electric potential travelling on magnetic surfaces in the direction y perpendicular to the field lines. Through the development of diverse types of micro-instabilities the wave amplitudes can grow in time. This growth introduces such a phase shift between density and potential perturbations so that the associated y-component of the electric field induces drift flows of particles and heat in the radial direction. These Anomalous flows tremendously enhance the level of losses due to classical and neoclassical transport contributions.

Different kinds of instabilities are of the most importance in the hot core and at the relatively cold edge of the plasma (Weiland, 2000). In the former case the so called toroidal ion temperature gradient (ITG) instability (Horton et all 1981) is considered as the most dangerous one. Spontaneous fluctuations of the ion temperature generate perturbations of the plasma pressure in the y-direction. These induce a diamagnetic drift in the radial direction bringing hotter particles from the plasma core and, therefore, enhancing the initial temperature perturbations. This mechanism is augmented by the presence of trapped electrons those can not move freely in the toroidal direction and therefore are in this respect similar to massive ions. On the one hand, the fraction of trapped particles is of $\sqrt{2r/(r+R)}$ and increases by approaching towards the plasma boundary. On the other hand, the plasma collisionality has to be low enough for the presence of "banana" trajectories. Therefore the corresponding instability branch, TE-modes (Kadomtsev & Pogutse, 1971), is normally at work in the transitional region between the plasma core and edge.

At the very edge the plasma temperature is low and coulomb collisions between electrons and ions are very often. They lead to a friction force on electrons when they move along the magnetic field in order to maintain the Boltzmann distribution in the perturbation of the electrostatic potential caused by a drift wave. As a result a phase shift between the density and potential fluctuations arises and the radial drift associated with the perturbed electric field brings particles from the denser plasma core. Thus, the initial density perturbation is enhanced and this gives rise to new branches of drift wave instabilities, drift Alfvén waves (DA) (Scott, 1997) and drift resistive ballooning (DRB) modes, see (Guzdar et al, 1993). The reduction of DA activity with heating up of the plasma edge is discussed as an important perquisite for the transition from the low (L) to high (H) confinement modes (Kerner et al, 1998). The development of DRB instability is considered as the most probable reason for the

density limit phenomena (Greenwald, 2002) in the L-mode, leading to a very fast termination of the discharge (Xu et al, 2003; Tokar, 2003).
Roughly the contribution from drift wave instabilities to the radial transport of charged particles can be estimated on the basis of the so called "improved mixing length" approximation (Connor & Pogutse, 2000):

$$D_{an} \approx \frac{\gamma_{\max}}{k_{y,\max}^2} \frac{\gamma_{\max}^2}{\gamma_{\max}^2 + \omega_{r,\max}^2} \tag{2}$$

Here γ and ω_r are the imaginary and real parts of the perturbation complex frequency, correspondingly; the former is normally refer to as the growth rate. Both γ and ω_r are functions of the y-component of the wave vector, k_y; the subscript "max" means that these values are computed at $k_y = k_{y,\max}$ at which γ approaches its maximum value. Such a maximum arises normally due to finite Larmor radius effects. For ITG-TE modes $k_{y,\max} \approx 0.3/\rho_{Li}$ and for DA-DRB drift instabilities $k_{y,\max} \approx 0.1/\rho_{Li}$, with ρ_{Li} being the ion Larmor radius.

1.3 Transitions between different transport regimes

Both the growth rate and real frequency of unstable drift modes and, therefore, the characteristics of induced anomalous transport depend in a complex non-linear way on the radial gradients of the plasma parameters. For ITG-TE modes triggered by the temperature gradients of ions and electrons, respectively, the plasma density gradient brings a phase shift between the temperature fluctuations and induced heat flows. As a result the fluctuations can not be fed enough any more and die out. For pure ITG-modes this impact is mimicked in the following simple estimate for the corresponding transport coefficient:

$$D_{an,ITG} \approx \frac{cT}{eBRk_{y,\max}} \sqrt{4\varepsilon_T - \varepsilon_n^2} \tag{3}$$

where $\varepsilon_{n,T} = R/(2L_{n,T})$ are the dimensionless gradients of the density and temperature, with $L_T = -T/\partial_r T$ and $L_n = -n/\partial_r n$ being the e-folding lengths of these parameters, correspondingly. Since the density profile is normally very peaked and ε_n is large at the plasma edge, ITG instability is suppressed in the plasma boundary region. Several sophisticated models have been developed to calculate firmly anomalous fluxes of charged particles and energy in tokamak plasmas (Waltz et al, 1997; Bateman et al, 1998). The solid curve in Fig. 2 shows a typical dependence on the dimensionless density gradient of the radial anomalous particle flux density computed by taking into account the contributions from ITG-TE modes calculated with the model from Ref. (Weiland, 2000), DA waves estimated according to Ref. (Kerner et al, 1998) and neoclassical diffusion from Ref. (Wesson, 2004), for parameters characteristic at the plasma edge in the tokamak JET (Wesson 2004): $R = 3\ m$, $r = 1\ m$, $B = 3\ T$, $n = 5 \cdot 10^{19}\ m^{-3}$, $T = 0.5\ keV$ and $L_T = 0.1\ m$. The dash-dotted curve provides the diffusivity formally determined according to the relation $D = -\Gamma/(dn/dr)$.
One can see that the total flux density Γ has an N-like shape. In stationary states the particle balance is described by the continuity equation $\nabla \cdot \Gamma = S$. Here S is the density of charged particle sources due to ionization of neutrals, entering the plasma volume through the separatrix, and injected with frozen pellets and energetic neutral beams. Since these sources

are, to some extent, in our hands, the stationary radial profile of the flux of charged particles can be also considered as prescribed. If at a certain radial position it is in the range $\Gamma_{\min} \le \Gamma \le \Gamma_{\max}$, see the thick dashed line in Fig.2, three steady states given by the black intersection points can be realized. They are characterised by very different values of the density gradient. The smallest gradient value corresponds to a very high particle transport and the largest one – to very low losses. In two neighbouring spatial points with close values of Γ the plasma can be in states belonging to different branches of the $\Gamma(\varepsilon_n)$ curve. Thus, a sudden change in the transport nature should happen between these points and this manifests itself in the formation of a transport barrier (TB).

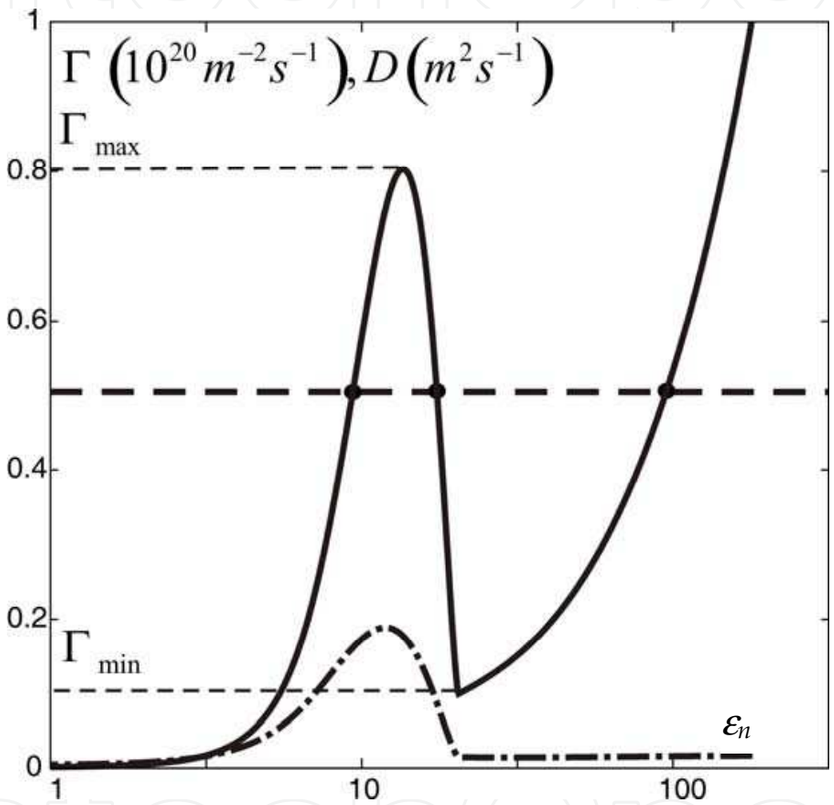

Fig. 2. The flux density (solid line) and diffusivity (dash-dotted line) of charged particles induced by unstable ITG, TE and DA modes and with neoclassical contribution

A stationary transport equation does not allow, nonetheless, defining uniquely the positions of the TB interfaces. This can be done only by solving non-stationary transport equations. Henceforth we consider this equation, applied to a variable Z, in a cylindrical geometry. After averaging over the magnetic surface it looks like:

$$\partial_t Z + \partial_r (r\Gamma)/r = S \tag{4}$$

In the present chapter it is demonstrated that this is not a straightforward procedure to integrate Eq.(4) with the flux density Γ being a non-monotonous function of the gradient $\partial_r Z$. Numerical approaches elaborated to overcome problems arising on this way are presented and highlighted below on several examples.

2. Numerical approach

2.1 Stability problems

For a positive dependence of the flux on the gradient, e.g. $\Gamma \sim (|\partial_r Z|)^p$ with $p > 0$, a numerical solution of Eq.(4) with a fully implicit scheme is absolutely stable for arbitrary time steps, see Ref. (Shestakov et al, 2003) . However for a non-monotonic dependence like that shown in Fig.1 there is a range with $p < 0$ and we have to analyze the numerical stability in this case. Let $\Psi(t,r)$ is the genuine solution of Eq.(4) with given initial and boundary conditions. Consider a deviation $\zeta(t,r)$ from $\Psi(t,r)$ that arises by a numerical integration of Eq.(4). By substituting $Z(t,r) = \Psi(t,r) + \zeta(t,r)$ into Eq.(4), we discretize linearly the time derivative, $\partial_t \zeta \approx [\zeta(t,r) - \zeta(t-\tau,r)]/\tau$. As a result one gets an ordinary differential equation (ODE) of the second order for the radial dependence of the variable ζ at the time moment $t = m\tau$, $\zeta_m(r)$. Not very close to the plasma axis, $r = 0$, we look for the solution of this equation in the form of plane waves (Shestakov et al, 2003):

$$\zeta_m = \lambda^m \exp(i\xi r) \tag{5}$$

with small enough wave lengths, $\xi >> |\Psi/\partial_r \Psi|$, $|\partial_r \Psi/\partial_r(\partial_r \Psi)|$. This results in:

$$\lambda \approx 1/\left(1 + \tau D p \xi^2\right) \tag{6}$$

where the diffusivity has been introduced according to the definition $D \equiv -\Gamma/\partial_r \Psi$. For a numerical stability $|\lambda| < 1$ is required. If $p > 0$, the absolute stability for any τ is recovered from Eq.(6), in agreement with Ref. (Shestakov et al, 2003). For negative p in question, $|\lambda| > 1$ and a numerical solution is unstable if

$$\tau < 2/\left(D|p|\xi^2\right) \tag{7}$$

i.e. for small enough time steps. Such instability was, most probably, the cause of problems arisen with small time steps by modelling of TB formation in Ref. (Tokar et al, 2006). It is also necessary to note that the approach elaborated in Ref. (Jardin et al, 2008) for solving of diffusion problems with a gradient-dependent diffusion coefficient and based on solving of a system of non-linear equations by iterations, does not work reliably as well in the situation in question: the convergence condition for a Newton-Raphson method used there is very easy to violate under the inequality (7). The limitation (7) on the time step does not allow following transport transitions in necessary details. Moreover, as it has been demonstrated in Ref. (Tokar, 2010), calculations with too large time steps can even lead to principally wrong solutions, with improper characteristics of final stationary states.

Thus, even in a normally undemanding one-dimensional cylindrical geometry normally used by modelling of the confined plasma region in fusion devices with numerical transport codes like JETTO (Cennachi& Troni, 1988), ASTRA (Pereverzev & Yushmanov, 1988), CRONOS (Basiuk et al, 2003), RITM (Tokar, 1994), it is not a trivial task to simulate firmly the time evolution of radial profiles if fluxes are non-monotonous functions of parameter gradients and transport bifurcations can take place. The development of reliable numerical schemes for such a kind of problems is an issue of permanent importance and has been tackled, in particular, in the framework of activities of the European Task Force on Integrated Tokamak Modelling (ITM, 2010).

2.2 Change of dependent variable

Analysis shows that problems with numerical stability considered above arise due to the contribution from the dependent variable at the previous time step, Z (t-τ,r), in the discretized representation of the time derivative in Eq.(4). Therefore one may presume that they can be avoided by the change to the variation of this variable after one time step, ξ (r) =Z(t,r) - Z(t-τ,r), proposed in Ref. (Tokar, 2010). However, it should be seen that such a change introduces into the source term on the right hand side (r.h.s.) a contribution from the flux divergence at the previous time moment. By calculating with large time steps, this contribution may be too disturbing and also lead to numerical instabilities. Therefore in the present study we suggest the change of variables in the following form:

$$\xi(r) = Z(t,r) - Z(t-\tau,r)\cdot \mathrm{e}^{-\tau/\tau_0} \tag{8}$$

where τ_0 is some memory time. In the limits of large, $\tau >> \tau_0$, and small, $\tau << \tau_0$, time steps, ξ (t,r) reproduces the representations of the dependent variable considered above, the original variable Z(t,r) and its variation after the time step Z(t,r) - Z(t-τ,r), respectively. As a result, with linearly discretized time derivative Eq.(4) takes the form:

$$\frac{\xi(r)}{\tau} + \frac{1}{r}\partial_r(r\Gamma) = S + Z(t-\tau,r)\frac{1-\mathrm{e}^{-\tau/\tau_0}}{\tau} \tag{9}$$

Due to nonlinear dependence of the flux density Γ on the density gradient the latter ODE have to be solved by iterations at any given time moment t. For a certain iteration level we represent Γ as a sum of diffusive and convective parts:

$$\Gamma = -D\cdot\partial_r Z + V\cdot Z \tag{10}$$

The diffusivity D(r) can be chosen in a form convenient for us. Then the convection velocity V(r) is determined from the requirement that the flux density Γ, found according to the transport model with the dependent variable Z at the previous iteration level, is reproduced by Eq.(10). This leads to:

$$V = \left(\Gamma_- + D\cdot\partial_r Z_-\right)/Z_- \tag{11}$$

An appropriate solver has to provide, of course, the same solution Z(t,r) independently of a choice for the diffusivity D(r).

For transport models, reproducing the formation of TB, we expect, at least in stationary states, a step-like change of the solution gradient at the position of the TB boundaries. Therefore such a discontinuity is also duplicated in the convection velocity V computed according to Eq. (11). As an alternative option, the situation with V = 0 but discontinuous D will be considered below. Such discontinuities in transport coefficients lead to difficulties by integrating Eq.(9): with the flux density represented by Eq.(10) it contains the radial derivatives of the transport coefficients D and V approaching to infinity at the position of the TB boundary. To avoid this we integrate Eq.(9), multiplied by r and obtain:

$$\frac{1}{\tau r}\int_0^r \xi\rho d\rho - D\cdot\partial_r\xi + V\cdot\xi = J \tag{12}$$

where

$$J=\frac{1}{r}\int_0^r\left[S+Z(t-\tau,r)\frac{1-\mathrm{e}^{-\tau/\tau_0}}{\tau}\right]\rho d\rho+\left[D\cdot\partial_r Z(t-\tau,r)-V\cdot Z(t-\tau,r)\right]\mathrm{e}^{-\tau/\tau_0} \tag{13}$$

Finally, an integral counterpart of the variable $\xi(r)$ is introduced:

$$y(r)=\frac{1}{r^2}\int_0^r\xi(\rho)\rho d\rho \tag{14}$$

and Eq. (12) is reduced to the second order ODE to y :

$$d^2y/dr^2+a\cdot dy/dr=by-f \tag{15}$$

with the coefficients $a=3/r-V/D$, $b=1/(\tau D)+2V/(rD)$ and $f=J/(rD)$.

Equation (15) has to be supplemented by boundary conditions. Due to axial symmetry the original variable Z has a zero derivative at the plasma axis, $r = 0$. From the relations above it follows that dy/dr also reduces to zero here. However, there is a singularity in Eq.(15) at $r = 0$ because the coefficient a becomes infinite here. Therefore, by a numerical realization the boundary condition has to be transferred to the point $r_1 > 0$. The error introduced by this procedure can be arbitrarily small by decreasing r_1. In the range $0 \le r \le r_1$ one can use the Taylor's expansion:

$$y(0\le r\le r_1)=y(r_1)+(r-r_1)\frac{dy}{dr}(r_1)+\frac{(r-r_1)^2}{2}\frac{d^2y}{dr^2}(r_1)$$

and the requirement $dy/dr\ (r = 0) =0$ reduces to:

$$r_1b(r_1)y(r_1)-\left[1+r_1a(r_1)\right]\frac{dy}{dr}(r_1)=r_1f(r_1) \tag{16}$$

The condition at the boundary of the confined plasma region, r_n , corresponds normally to a prescribed value of the variable Z or its e – folding length, $-dr/d\ (\ln Z)= \delta$. In the latter case we get for the variable y:

$$\left[r_n/\tau+2(D/\delta+V)\right]y+r_n(D/\delta+V)\cdot dy/dr=J \tag{17}$$

2.3 Numerical solution

The coefficients in Eq.(15) are finite everywhere but discontinuous at the boundaries of a TB. Therefore, by integrating it, one can run to difficulties with applying established approaches, e.g., finite difference, finite volume and finite element methods, see Refs. (Versteeg & Malalasekera, 1995; Tajima, 2004; Jardin, 2010). In these approaches the derivatives of the dependent variable are discretized on a spatial grid with knots $r_{1,\ldots,n}$. This procedure implies a priory a smooth behaviour of the solution in the vicinity of grid knots. Usually it is supposed that this can be described by a quadratic or higher order spline. However, in the situation in question we expect a discontinuity of the derivative of y due to discontinuous transport coefficients. Thus, by following Ref. (Tokar, 2010), Eq.(15) is

approximated in the vicinity $r_i^- \le r \le r_i^+$ of the grid knots i =2,...n-1, with $r_i^{\pm} = (r_{i\pm1} + r_i)/2$, by the second order ODEs with constant coefficients $a = a_i \equiv a(r_i)$, $b = b_i \equiv b(r_i)$, and $f = f_i \equiv f(r_i)$. Exact analytical solutions of such equations are given as follows:

$$y^i(r) = y\left(r_i^- \le r \le r_i^+\right) = C_{i,1}y_{i,1}(r) + C_{i,2}y_{i,2}(r) + y_{i,0} \tag{18}$$

The discriminant of Eq.(15) is positive. Indeed,

$$\Delta = \frac{a^2}{4} + b = \frac{1}{4}\left(\frac{3}{r} - \frac{V}{D}\right)^2 + \frac{1}{\tau D} + \frac{2V}{rD} = \frac{2}{r^2} + \frac{1}{4}\left(\frac{1}{r} + \frac{V}{D}\right)^2 + \frac{1}{\tau D} > 0$$

Thus the general solutions in Eq.(18) are exponential functions, $y_{i,k=1,2} = \exp\left[\lambda_{i,k}(r - r_i)\right]$, with $\lambda_{i,k} = -a_i/2 - (-1)^k\sqrt{\Delta(r_i)}$; the partial solution we chose in the form $y_{i,0} = f_i/b_i$. The continuity of the solution and its first derivative at the interfaces $r_i^{\pm}$ of the grid knot vicinities allow to exclude the coefficients $C_{i,k}$ and to get a three-diagonal system of linear equations for the values y_i of the solution in the grid knots:

$$y_i = y_{i-1}g_{i,1} + y_{i+1}g_{i,2} + \chi_i$$

where $g_{i,k}$ and χ_i are expressed through $y_{i,k}(r_i^{\pm})$, $y_{i,0}$ and $\lambda_{i,k}$, see Ref. (Tokar, 2010) for details. These equations have to be supplemented by the relations following from the boundary conditions (16) and (17) where the approximations $dy/dr\ (r_1) \approx (y_2 - y_1)/(r_2 - r_1)$ and $dy/dr\ (r_n) \approx (y_n - y_{n\text{-}1})/(r_n - r_{n\text{-}1})$ are applied.

With $y_{1,\ldots,n}$ known, the original dependent variable $Z(t,r)$ is determined by using the relations (8) and (14):

$$Z(t,r) = Z(t-\tau,r)\cdot \mathrm{e}^{-\tau/\tau_0} + 2y + r\,dy/dr \tag{19}$$

One can see, $Z(t,r)$ is defined through both y and its derivative. Since the latter changes abruptly at the TB border, it is essential to calculate dy/dr as exact as possible, i.e. by using the expression (18) directly:

$$dy/dr(r_i) = C_{i,1}\lambda_{i,1} + C_{i,2}\lambda_{i,2}$$

Finally a new estimation for the transport coefficients is calculated with the new approximation to the solution $Z(t,r)$. Normally it is, however, necessary to use a stronger relaxation by applying some mixture of the old approximation, with the subscript (-), and the new one marked by the subscript (+). For example, for the convection velocity we have:

$$V = V_- \cdot (1 - A_{mix}) + V_+ \cdot A_{mix}$$

For the given time moment iterations continue till the convergence criterion:

$$\text{Error} = \sqrt{\sum_i \left[V_-(r_i) - V_+(r_i)\right]^2 \Big/ \sum_i \left[V_-(r_i) + V_+(r_i)\right]^2} \le 10^{-5} A_{mix}$$

is fulfilled.

3. Examples of applications

3.1 Temperature profile with the edge transport barrier

The most prominent example of TB in fusion tokamak plasmas is the edge transport barrier (ETB) in the H-mode with improved confinement (Wagner et al, 1982). The ETB may be triggered by changing some controlling parameters, normally by increasing the heating power (ASDEX Team, 1989). It is, however, unknown *a priory* when and where such a transport transition, inducing a fast modification of the parameter profiles, can happen. Regardless of the long history of experimental and theoretical studies, it is still not clear what physical mechanisms lead to suppression of anomalous transport in the ETB. The main line of thinking is the mitigation of drift instabilities and non-linear structures, arising on a non-linear stage of instabilities, through the shear of drift motion induced by the radial electric field (Diamond 1994, Terry 2000). Other approaches speculate on the role of the density gradient at the edge in the suppression of ITG-TE modes (Kalupin et al, 2005) and reduction of DA instabilities with decreasing plasma collisionality (Kerner, 1998; Rogers et al, 1998; Guzdar, 2001), the sharpness of the safety factor profile in the vicinity of the magnetic separatrix in a divertor configuration, etc. To prove the importance of a particular physical mechanism, the ability to solve numerically heat transport equations, allowing the formation of ETB, and to calculate the time evolution of the plasma parameter profiles is of principle importance.

Henceforth we do not rely on any particular mechanism for the turbulence and anomalous transport suppression but take into account the fact that in the final state the plasma core with a relatively low temperature gradient, $\partial_r T$, co-exists with the ETB where the temperature gradient is much larger. Since there are no any strong heat sources at the interface between two regions, the strong discontinuity in $\partial_r T$ is a consequence of an instantaneous reduction in the plasma heat conduction κ. Most roughly such a situation is described as a step-like drop of κ if $|\partial_r T|$ exceeds a critical value $|\partial_r T|_{cr}$. For convenience, however, we adopt that this happens if the e-folding length L_T drops below a certain L_{cr} ; κ is equal to constant values κ_0 for $L_T > L_{cr}$ and $\kappa_1 << \kappa_0$ for $L_T < L_{cr}$, see Fig.3.

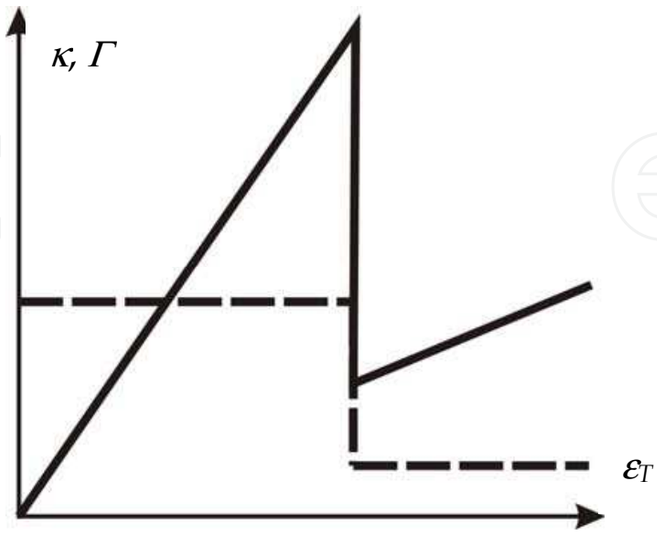

Fig. 3. Step-model for heat conduction (dashed line) and flux density (solid line) dependence on the dimensionless temperature gradient

The temperature profile $T(r)$ is described by Eq. (4) and it is assumed that the source density S is independent of the time and radial position. First consider stationary states with $\partial T/\partial t = 0$. In this case the heat flux density increases linearly with the radius, $\Gamma = Sr/2$. The corresponding radial profiles can be found analytically if one accepts that the transition from the strong transport in the plasma core, $\kappa = \kappa_0$, to the low transport at the edge, $\kappa = \kappa_1$, occurs at a position r_*. The existence of a central region with intense transport is ensured by the fact that L_T is infinite at the plasma axis, $r = 0$, where $\partial T/\partial r = 0$. At the boundary r_n we fix the temperature $T(r_n) = T_1$. The latter is governed by transport processes outside the last closed flux surface, in the scrape-off layer (SOL), where magnetic field lines hit a material surface. Stationary temperature profiles are given as follows:

$$\begin{aligned} T\left(0 \le r \le r_*\right) &= \frac{S}{4}\left(\frac{r_*^2 - r^2}{\kappa_0} + \frac{r_n^2 - r_*^2}{\kappa_1}\right) + T_1 \\ T\left(r_* \le r \le r_n\right) &= \frac{S}{4}\frac{r_n^2 - r^2}{\kappa_1} + T_1 \end{aligned} \tag{20}$$

At the position of the interface between the region of strong transport and the ETB the heat flux density $\Gamma(r_*)$ should be in the range where its dependence on the temperature e-folding length is ambiguous, i.e. the following inequalities have to be satisfied:

$$\frac{\kappa_1 T\left(r_*\right)}{L_{cr}} \le \frac{S r_*}{2} \le \frac{\kappa_0 T\left(r_*\right)}{L_{cr}}$$

These give quadratic equations for the upper and lower boundaries of the interface position r_*. From these equations one gets the range of possible positions of the ETB interface:

$$r_*^{\min} \equiv \sqrt{L_{cr}^2 + r_n^2 + 4\kappa_1 T_1/S} - L_{cr} \le r_* \le \sqrt{\left(L_{cr}\,\kappa_1/\kappa_0\right)^2 + r_n^2 + 4\kappa_1 T_1/S} - L_{cr}\,\kappa_1/\kappa_0 \equiv r_*^{\max} \tag{21}$$

For the existence of ETB the lower limit has to be smaller than r_n. In agreement with observations this results in the requirement that the heating power has to exceed a minimum value:

$$S \ge S_{\min} \equiv 2\kappa_1 T_1/\left(r_n L_{cr}\right) \tag{22}$$

The stationary analysis above does not allow fixing the position of the interface between regions with different transport levels and for this purpose the non-stationary equation (4) has to be solved. This is done for different initial conditions in the form:

$$T\left(0, r\right) = T_1 + \alpha\frac{S}{4}\frac{r_n^2 - r^2}{\kappa_1}$$

By increasing the factor α one can reproduce different situations from a flat initial profile $T(r) = T_1$ for $\alpha = 0$ with very small thermal capacity, to a very peaked temperature for $\alpha > 1$ with a total thermal energy exceeding that in any stationary state. Calculations were done with the parameters $\kappa_1/\kappa_0 = 0.1$ and $L_{cr}/r_n = 1$. Only these combinations are of importance by calculating the dimensionless temperature $\Theta = \kappa_0 T/(Sr_n^2)$ as a function of the dimensionless

radius $\rho = r/r_n$ and time $t/(r_n\kappa_0)$. The boundary condition Θ (ρ = 1) =0.01 ensures the existence of an ETB. The stationary profiles obtained by a numerical solution of the time-dependent equation with the time step $\tau = 10^{-3}/(r_n\kappa_0)$, the memory time $\tau_0 = 10^3\tau$ and an equidistant spatial grid with the total number of points n = 500 are shown in Fig.4 for different magnitudes of the parameter α. The analytical profiles (20) with r_* obtained from the numerical solutions are presented by thick bars. One can see a perfect agreement between analytical and numerical solutions and that the total interval $r_*^{\min} \le r_* \le r_*^{\max}$ can be realized by changing the steepness α of the initial temperature profile. It is also important to notice that only for sufficiently small τ and large τ_0 calculations provide the same final profiles. Thus, it is of principal significance to make the change of variable according to the relation (8) and operate with the temperature variation after a time step but not with the temperature itself. Finally we compare the results above with those obtained by the method described in Ref. (Tokar, 2006b), which has been also applied to non-linear transport models allowing bifurcations resulting in the ETB formation. Independently of initial conditions and time step this method provides final stationary states with the TB interface at $r_* = r_*^{\max}$. In Ref. (Tokar, 2006b) the solution was found by going from the outmost boundary, $r = r_n$, where the plasma state is definitely belongs to those with the low transport level. If in the point r_{i-1} solutions with three values of the gradient are possible, see Fig.2, the one with the gradient magnitude closest to that in the point r_i has been selected. This constraint is, probably, too restrictive since it allows transitions between different transport regimes only in points where the optimum flux values $\Gamma_{\min}$ and $\Gamma_{\max}$ are approached.

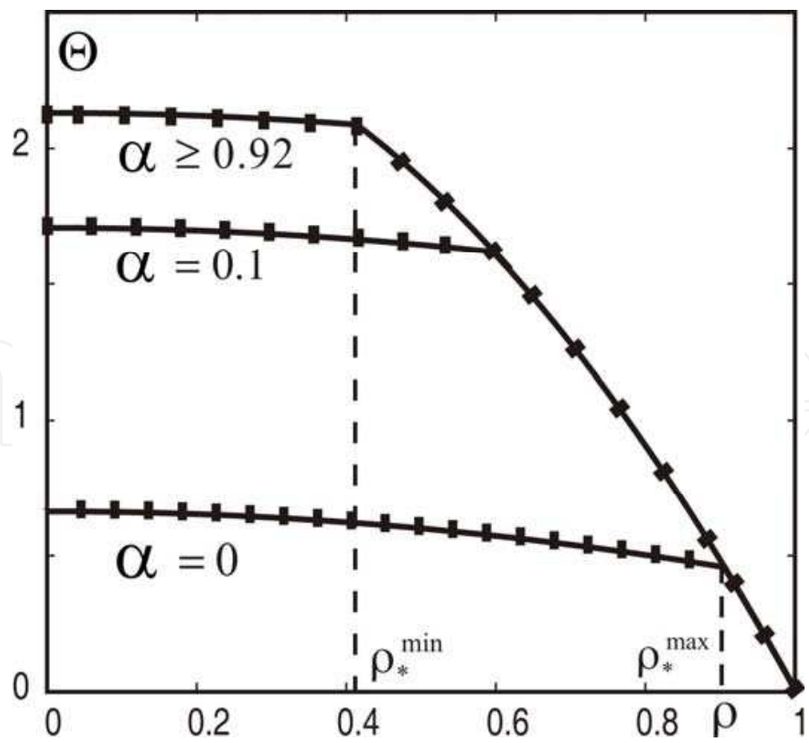

Fig. 4. Final stationary temperature profiles computed with differently peaked initial profiles

As another example we consider a plasma with a heating under the critical level where the formation of ETB is paradoxically provoked by enhanced radiation losses from the plasma edge. In fusion devices such losses are generated due to excitation by electrons of impurity particles eroded from the walls and seeded deliberately for diverse purposes. Normally radiation losses lead to plasma cooling and reduction of the temperature (Wesson, 2004). However, under certain conditions an increasing temperature has been observed under impurity seeding (Lazarus et al, 1984; Litaudon et al, 2007). Usually effects of impurities on the anomalous transport processes, in particular through a higher charge of impurity ions compared with that of the main particles, is discussed as a possible course of such a confinement improvement (Tokar, 2000a). Particularly it has been demonstrated that ITG-instability can be effectively suppressed by increasing the ion charge. Here, however, we do not consider such effects but take into account radiation energy losses in Eq.(4) by replacing the heat source S with the difference S-R, where R is the radiation power density. The latter is a non-linear function of the electron temperature and for numerical calculations in the present study we take it in the form (Tokar, 2000b):

$$R = R_0(t) \cdot \exp\left[-\left(\sqrt{\frac{T_{\min}}{T}} - \sqrt{\frac{T}{T_{\max}}} \right)^2 \right] \tag{23}$$

The factor R_0 is proportional to the product of the densities of radiating impurity particles and exciting electrons. The exponent function takes into account two facts: (i) for temperatures significantly lower than the level $T_{\min}$ electrons can not excite impurities and (ii) for temperatures significantly exceeding $T_{\max}$ impurities are ionized into states with very large excitation energies. For neon, often used in impurity seeding experiments (Ongena, 2001), $T_{\min}$ is of several electron-volts and $T_{\max} \approx 100\ eV$, see Ref.(Tokar, 1994). Thus the radiation losses are concentrated at the plasma edge where the temperature is essentially smaller than several keV typical for the plasma core.

Why additional energy losses with radiation can provoke the formation of ETB? Consider stationary temperature profile in the edge region where the heating can be neglected compared with the radiation, i.e. $T_{\min} < T < T_{\max}$. By approximating R with R_0, the heat transport equation is reduced to the following one:

$$\kappa d^2T/dx^2 \approx R_0 \tag{24}$$

where $x = r_n - r$ is the distance from the LCMS. This equation can be straightforwardly integrated leading to:

$$\frac{dT}{dx} \approx \frac{R_0}{\kappa} x + \frac{T(0)}{\delta}, \; T \approx \frac{R_0}{\kappa} \frac{x^2}{2} + T(0) \cdot \left(\frac{x}{\delta} + 1 \right) \tag{25}$$

The temperature value at the LCMS, $T(0)$, has to be found from the conditions at the inner boundary of the radiation layer, $x = x_{rad}$, where $T \approx T_{\max}$ and the heat flux density from the core, $\kappa\, dT/dx$, is equal to the value q_{heat} prescribed by the central heating. The plane geometry adopted in this consideration implies $x_{rad} << r_n$. From Eqs.(25) one finds:

$$L_T = \frac{\chi^2 \gamma_{rad}/2 + (\chi + \delta/x_{rad})(1 - \gamma_{rad})}{\chi \gamma_{rad} + 1 - \gamma_{rad}} \tag{26}$$

where the dimensionless co-ordinate $0 \le \chi \equiv x/x_{rad} \le 1$ and radiation level $\gamma_{rad} \equiv R_0 x_{rad}/q_{heat}$ are introduced. For δ/x_{rad} and γ_{rad} large enough the χ-dependence of the r.h.s. in Eq.(26) is non-monotonous: with χ increasing from zero it first goes down and then up. Qualitatively the decrease of L_T means that if the heat contact with the SOL-region out of the confined plasma is weak, i.e. δ is large, the radiation losses lead to a stronger decrease of the temperature than of the conductive heat flux in the radiation layer. At the plasma boundary, $x = 0$, we assume $L_T = \delta > L_{cr}$, i.e. there is no ETB without radiation. With radiation the condition for the transport reduction, $L_T < L_{cr}$, can be, however, fulfilled somewhere inside the radiation layer, $0 < x < x_{rad}$.

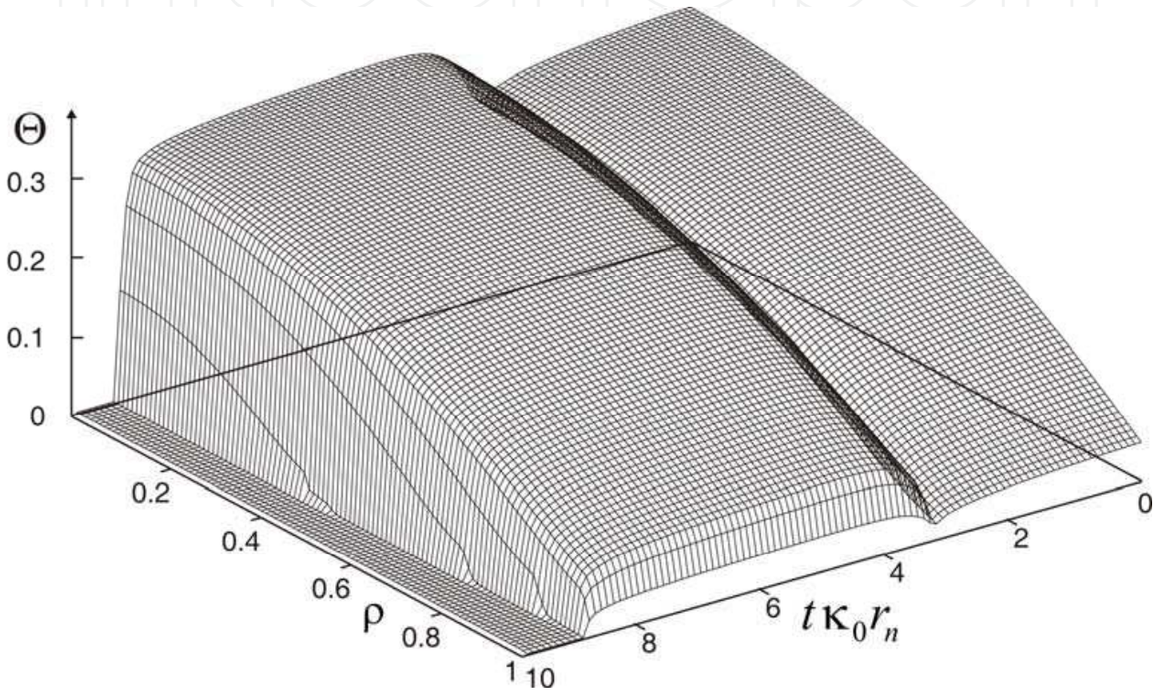

Fig. 5. The time evolution of the temperature profile under conditions of sub-critical heating with the ETB formation induced by the radiation energy losses increasing linearly in time. Finally the radiation triggers plasma collapse

If the radiation intensity is too high the state with the radiation layer at the plasma edge does not exist at all. This can be seen if, by using Eqs.(25) and the conditions at the inner interface of the radiation zone with the plasma core, one calculates $T(0)$:

$$T(0) = \left(R_0\delta \pm \sqrt{R_0^2\delta^2 + q_{heat}^2 - 2\kappa R_0 T_{\max}} \right) \delta/\kappa \tag{27}$$

If the discriminant in Eq.(27) is positive, as it is the case for R_0 small enough, there are two values for $T(0)$ but only the state with the edge temperature given by Eq.(27) with the sign (+), i.e., with larger $T(0)$, is stable. Indeed, in the state with (-) in Eq.(27) and smaller $T(0)$ the total energy loss increases with decreasing $T(0)$. If the temperature spontaneously drops, the radiation layer widens and the radiation losses grow up leading to a further drop of $T(0)$. With increasing R_0 the discriminant approaches to its minimum level $q_{heat}^2 - \left(\kappa T_{\max}/\delta\right)^2$

at $R_0 = \kappa T_{\max}/\delta^2$. If the flux from the plasma core is smaller than the critical value $\kappa T_{\max}/\delta$, there are no stationary states at all with the radiation layer located at the plasma edge if R_0 exceeds the level:

$$R_0^{\max} = \left(1 - \sqrt{1 - q_{heat}^2 \delta^2 / \kappa^2 T_{\max}^2}\right) \kappa T_{\max}/\delta^2 \tag{28}$$

In such a case the radiation zone spreads towards the plasma core and a radiation collapse takes place. Figure 5 demonstrates the corresponding time evolution of the radial profile for the dimensionless temperature Θ found from Eq.(4) with the radiation losses computed according to Eq.(3) where the amplitude grows up linearly in time, $R_0(t) \sim t$. As the initial condition a stationary profile in the state without any radiation and ETB ($\delta > L_{cr}$), has been used. One can see that at a low radiation the total temperature profile is first settled down with increasing R_0. However, at a certain moment a spontaneous formation of the ETB takes place. The ETB spreads out with the further increase of the radiation amplitude. When the latter becomes too large radiation collapse develops.

3.2 Time evolution of the plasma density profile

As the next example the evolution of the plasma density profile by an instantaneous formation of the ETB will be considered. This evolution results from the interplay between transport of charged particles and their production due to diverse sources in fusion plasmas. Normally the most intensive contribution is due to ionization of neutral particles which are produced by the recombination on material surfaces of electrons and ions lost from the plasma. If the surfaces are saturated with neutral particles they return into the plasma in the process of "recycling" (Nedospasov & Tokar, 2003). Thus the densities of neutral atoms, n_a, and charged particles, n, are interrelated and the source term in Eq.(4) for charged particles, $S = k_{ion} n n_a$, where k_{ion} is the ionization rate coefficient, depends non-linearly on n. This non-linearity may be an additional cause for numerical complications. The transport of recycling neutrals is treated self-consistently with that of charged particles and n_a is determined by the continuity equation:

$$\partial_t n_a + 1/r \cdot \partial_r \left(r j_a\right) = -S \tag{29}$$

with the flux density j_a computed in a diffusive approximation, see, e.g., (Tokar, 1993) :

$$j_a = -\frac{T_a}{m_a \left(k_{ion} + k_{cx}\right) n} \partial_r n_a \tag{30}$$

This approximation takes into account that the rate coefficient for the charge-exchange of neutrals with ions, k_{cx}, is noticeably larger than k_{ion}. Thus, before the ionization happens neutrals charge-exchange with ions many times and change their velocities chaotically, i.e., a Brownian like motion takes place. At the entrance to the confined plasma, $r = r_n$, the temperature T_a of recycling neutrals is normally lower than that of the plasma, $T_a(t, r = a) < T(t, r = a)$. However after charge-exchange interactions the newly produced atoms acquire the ion kinetic energy and T_a approaches to T. This evolution is governed by the heat balance equation:

$$n_a \partial_t T_a + j_a \partial_r T_a = k_{cx} n n_a \left(T - T_a\right) \tag{31}$$

By discretizing this in time and in space, one gets the following recurrent relation:

$$T_{a,i} = \frac{n_{a,i}T^{-}_{a,i}/\tau - j_{a,i}T_{a,i+1}/(r_{i+1}-r_i) + (k_{cx}nn_aT)_i}{n_{a,i}/\tau - j_{a,i}/(r_{i+1}-r_i) + (k_{cx}nn_a)_i}$$

allowing to calculate the atom temperature profile at the time moment t, $T_{a,i<n} \equiv T_a\left(t, r_{i<n}\right)$, from that at the previous time t - τ, $T^{-}_{a,i<n} \equiv T_a\left(t-\tau, r_{i<n}\right)$, and boundary condition $T_{a,n} \equiv T_a\left(t, r_n\right)$. In this consideration we assume that the radial profile of the plasma temperature T, assumed the same for electrons and ions, is prescribed as follows:

$$T(r) = T(0) - \left[T(0) - T(r_n)\right](r/r_n)^2 \tag{32}$$

Figure 6 shows the time evolution of the central plasma density, $n(t,r = 0)$, computed for the conditions of the tokamak TEXTOR (Dippel et al, 1987) with the minor radius of the LCLS r_n = 0.46 m, the central plasma temperature $T(0)$ =1.5 keV and the following parameters at the LCMS: the plasma temperature, $T(r_n)$ =50 eV , the neutral density $n_a(r_n)$ =$2\cdot10^{16}m^{-3}$ and temperature $T(r_n)$ = 25 eV. The initial profile of the plasma density was assumed parabolic and given by a formula similar to Eq.(32) with the values at the axis $n(0)$ =$5\cdot10^{19}m^{-3}$ and at the LCMS $n(r_n)$ =$10^{19}m^{-3}$, respectively. To investigate the impact of nonlinearities introduced by the coupling of the densities of neutral and charged particles only, these computations have been done for a smooth radial variation of the plasma particle diffusivity D also given by a formula similar to Eq.(32) with D(0)=$0.2m^2s^{-1}$ and $D(r_n)$ =$0.8\ m^2s^{-1}$ and zero convection velocity V.

Different panels and curves in Fig.6 show the results obtained for different time steps τ and memory times τ_0. One can see in Fig.6a that for $\tau_0 << \tau$ problems arise by computing with small τ. This happens in spite of the fact that the calculations were done with particle transport characteristics independent of the density gradient, i.e. p = 1 in the flux dependence on $\partial_r n$, see page 3. The reason for such behaviour can be the non-linearity in the source S due to the ionization of neutrals and the involvement of the solution at the previous time moment t - τ into the inhomogeneous term f in Eq.(15) for the variable y. Indeed, for $\tau_0 << \tau$ this contribution is given by the integral from $n(t-\tau,r)/\tau$ that becomes unboundedly large with decreasing time step. As a result a large error can accumulate after many time steps and no stationary state is achieved for $\tau = 10^{-4}$s and $\tau_0 = 10^{-6}$s.

The behaviour described above contradicts both physical expectations and the existence of stationary analytical solution found for a plane geometry approximation applicable for the neutral penetration depth significantly less than the plasma radius r_n, and with the plasma diffusivity D and particle temperatures T, T_a constant along the radius, see, e.g., Ref. (Tokar 1993). Under these conditions one can introduce the dimensionless co-ordinate

$$u = \int_r^{r_n} \sigma_* n d\rho$$

where $\sigma_* = \sqrt{m_a k_{ion}\left(k_{ion} + k_{cx}\right)/T_a}$ is the effective cross-section for the attenuation of neutrals in the plasma,. With this variable change Eqs. (29), (30) are reduced to a very simple one:

$$d^2 n_a / du^2 = n_a$$

and the physically meaning solution, decaying towards the plasma core, is:

$$n_a \approx n_a(r_n)\cdot\exp(-u)$$

Then the stationary continuity equation for charged particles is as follows:

$$d^2u/dr^2 = \exp(-u)\cdot n_a(r_n)k_{ion}/D$$

By multiplying both sides of the latter with $2du/dr$, we get after a straightforward integration:

$$n(u) \equiv \frac{1}{\sigma_*}\frac{du}{dr} = \frac{1}{\sigma_*}\sqrt{\left[\delta\frac{n_a(r_n)k_{ion}}{D}\right]^2 + 2\frac{n_a(r_n)k_{ion}}{D}\left[1-\exp(-u)\right]}$$

where to determine the integration constant we have used the boundary condition at the LCMS, $dn/dr = -n/\delta$. The explicit dependences $u(r)$ and $n(r)$ can be obtained from this relation, see, e.g., Ref. (Tokar, 1993), by using table of integrals (Gradshteyn & Ryzhik, 1965). Interesting that the latter one reproduces hyperbolic tangent law often used to approximate experimentally found density profiles.

The solution is stable if τ is increased, however, the larger the time step the more details of the time dynamics are lost. Figure 6b demonstrates the results found for $\tau << \tau_0 = 10s$. In this case calculations with all $\tau < 1s$ are numerically stable and result in the same final stationary value of the central density of $5.4\cdot10^{19}m^{-3}$. Nonetheless, a numerical instability reappears again for τ exceeding some critical value of $1s$. A probable reason for this behaviour is again the involvement of the solution at the previous time moment into the term J in Eq.(13). Now the problem arises because of two last two terms in J which do not become smaller with increasing τ as this is the case for the integral contribution. For large time steps these terms are dubious. Improper impacts of the solution at the previous time in Eq.(15) can be avoided if the memory time τ_0 is suitably chosen. In Fig.6c we show the time behaviour of $n(t,r=0)$ found with $\tau_0 = 1s$. The solutions have similar time evolution for any τ, as one may expect for a given time step, and approach to the same stationary value of $5.4\cdot10^{19}m^{-3}$.

It is not obviously how to choose a proper τ_0 in a particular situation. The consideration above indicates that for small time steps the second term under the integral in J, Eq.(13), has not to exceed the last two contributions and for large τ the ordering has to be opposite. As a rough condition satisfying both constraints one can adopt the equality of these terms averaged over the whole computation domain. This results in:

$$\tau_0 = \frac{\tau}{\ln(1+\tau/\tau_c)} \tag{33}$$

where the "confinement" time is defined as follows:

$$\tau_c = \frac{1}{r_n\Gamma(r_n)}\int_0^{r_n} n(t-\tau,r)\,r\,dr$$

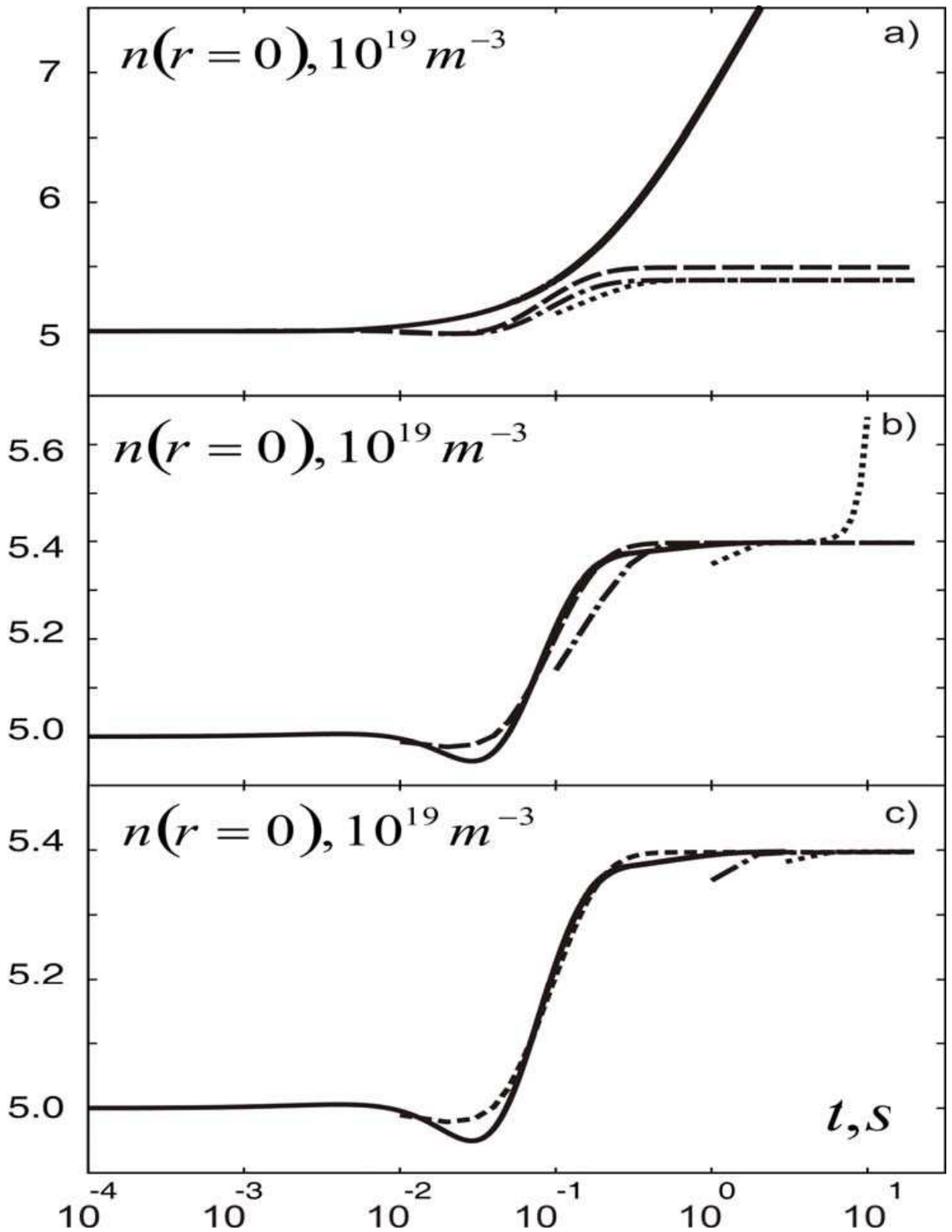

Fig. 6. The time evolution of the central plasma density computed with different memory times and time steps: $\tau_0 = 10^{-6}$ *s* , $\tau = 10^{-4}$ *s* (solid line), 10^{-3} s (dashed line), 10^{-2} *s* (dash-dotted line) and 10^{-1} *s* (dotted line) (a) ; $\tau_0 = 10$ *s* , $\tau = 10^{-4}$ *s* (solid line), 10^{-2} *s* (dashed line), 10^{-1} *s* (dash-dotted line) and 1*s* (dotted line) (b); $\tau_0 = 1$ *s* , $\tau = 10^{-4}$ *s* (solid line), 10^{-2} *s* (dashed line), 1*s* (dash-dotted line) and 3 *s* (dotted line) (c). All curves begin after the first time step, at $t = \tau$

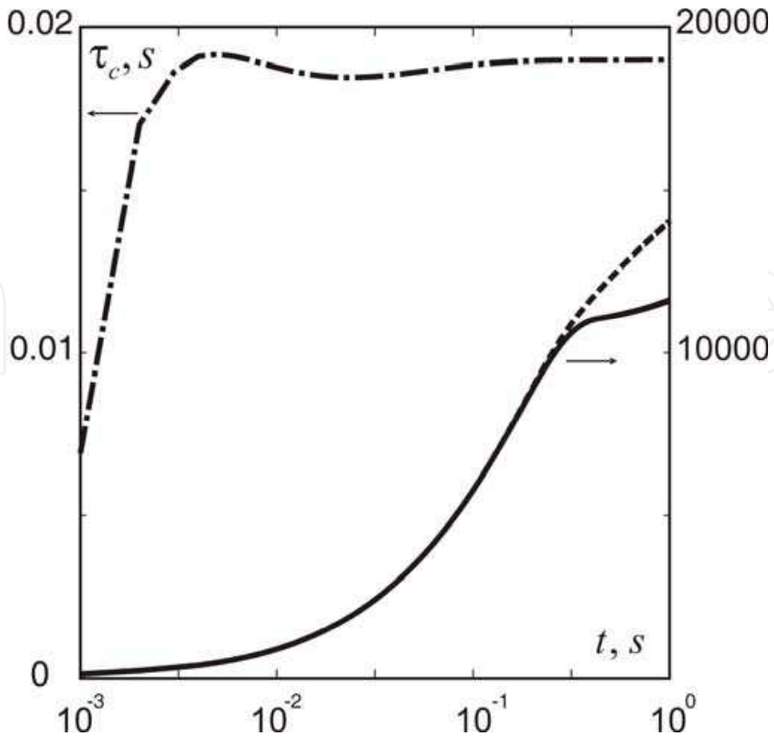

Fig. 7. The number of iterations done to the time t by calculating with the fixed memory time τ_0 (dashed curve), with the optimized one calculated according to Eq.(33) (solid line) and the time variation of the confinement time τ_c (dash-dotted line)

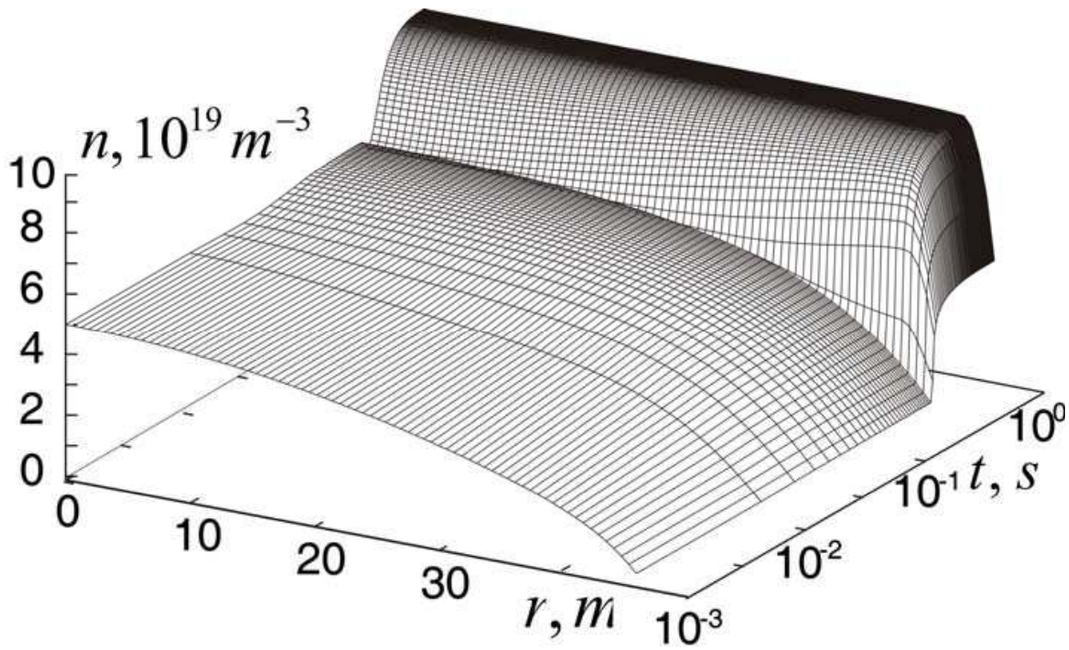

Fig. 8. The time evolution of the plasma density profile with formation of the ETB computed with $\tau = 10^{-3}$ s and τ_0 defined according to Eq.(33)

In the limit cases, $\tau << \tau_c$ and $\tau_c << \tau$ we have $\tau_0 \approx \tau_c$ and $\tau_0 \approx \tau/\ln(\tau/\tau_c)$, respectively. Figure 7 shows the time variation of τ_c for the density evolution calculated with $\tau = 10^{-3}s$ and $\tau_0 = 1s$. Also the number of iterations done to the time t by computations with $\tau_0 = 1s$ and with τ_0 determined according to Eq.(33) are demonstrated. One can see that in the latter case the number of iterations decreases significantly by approaching to the steady state at large t.

The estimate (33) gives a good hint for a proper memory time also in calculations with the formation of transport barriers. The results of this calculation are demonstrated in Fig.8 showing the time evolution of the density profile obtained by assuming that at time $t = 0.3\ s$ there is an instantaneous reduction by a factor of 10 of the charged particle diffusivity D in the edge region $r_n - \Delta \le r \le r_n$ with $\Delta = 0.02\ m$. In this case computations with $\tau_0 > > 0.5$ s, i.e. significantly exceeding τ_c, are unstable.

4. Conclusion

Transport processes in fusion plasmas can be caused by diverse physical mechanisms. The most straightforward one is due to Coulomb collisions between charged particles. Due to conservation of momentum collisions provoke a net particle displacement only by interactions of particles of opposite charges, i.e. electrons and ions. For such a classical diffusion the characteristic mean free path is of the electron Larmor radius and the level of induced particle losses is very low. In a tokamak with curved magnetic field lines these losses are enhanced significantly by the drift motion originated from the field inhomogeneity and curvature of field lines. Nonetheless, the corresponding so called neo-classical transport does not provide obstacles to confine and heat plasmas to thermonuclear temperatures. Much more dangerous are innumerable drift instabilities triggered by sharp gradients of the plasma parameters in the radial direction across the magnetic surfaces. These instabilities enhance anomalously, by orders of magnitude, the particle and energy losses over the neoclassical level. Different types of such instabilities are of importance in the hot core and at the relatively cold edge of the plasma. In the core instabilities triggered by the radial temperature gradients, namely, ion temperature gradient and collisionless trapped electron modes are of the most importance. At the edge where coulomb collisions are often enough drift Alfvén waves and drift resistive ballooning modes may be dominant. Important characteristics of unstable modes, e.g., growth rates are essentially dependent on the plasma parameter gradients. Therefore some instability can be completely suppressed if certain critical gradients are approached. As a result the induced fluxes of particles and energy are non-linear non-monotonous functions of the gradients. Such behaviour results in an ambiguity of local gradient values in stationary states and provides possibilities for bifurcations like the formation of transport barriers.

It is demonstrated that in the case of fluxes decaying with increasing gradient the numerical solution of a diffusion-like equation is unstable for time steps smaller than a critical one. This does not allow describing time dynamics of transport transitions in necessary details and leads even to principally wrong plasma final states resulting from this calculation. An approach based on a proper change of dependent variable proposed in the present chapter allows avoiding difficulties outlined above. It includes several principal elements: (i) change over to a new dependent variable ξ relating the values of the original one Z at the present and previous time moments through the time step and a memory time τ_0, (ii) transition to an

integral form of the primary equation and change to an integral counterpart y of the variable ξ and (iii) approximation of the second order ODE for y in the vicinities of grid knots by ODEs with constant coefficients whose exact analytical solutions are conjugated by requiring the continuity of the solution and its first spatial derivative.

The approach elaborated is demonstrated by modelling of the development of the edge transport barrier in a tokamak. The plasma heat conduction dependence on the temperature gradient is assumed as a dropping abruptly at a critical value of the temperature *e*-folding length. First a situation with a heating exceeding a critical level is considered that corresponds to a L_T magnitude at the LCMS smaller than L_{cr}. Calculations have shown that, depending on the initial temperature profile, the whole range of the radial position of the interface between ETB and the core region with strong transport, predicted by an analytical model, can be realized in the final stationary state. Computations also demonstrate that an ETB can be triggered even with a subcritical heating if impurity radiation localized at the very plasma edge is enhanced to a certain critical level. This may improve the understanding of the radiation improved mode observed in several tokamaks.

Modelling of the plasma density profile involves additional non-linearity through the coupling between the densities of charged and neutral particles. This can lead to numerical instabilities in calculations with both too small and too large memory times. With a proper chosen τ_0 such difficulties can be avoided. An approach is proposed to choose the memory time. Itis based on the equilibration of different contributions to the free term in the equation for y and relates τ_0 to the confinement time. The optimization of the τ_0 selection procedure allows reducing noticeably the total number of iterations required to achieve the stationary solution. It allows also modelling reliably the plasma density evolution by a spontaneous formation of the ETB. The methods developed can be applied by simulations of other physical phenomena in fusion plasmas having a bifurcation-like character, e.g., density limits, and phase transitions in other media.

5. References

ASDEX Team (1989) The H-mode in ASDEX , *Nucl. Fusion* Vol. 29, No. 11 (November 1989), pp. 1959—2040, ISSN 0029-5515

Basiuk, V. et al (2003) Simulations of steady-state scenarios for Tore Supra using the CRONOS code, *Nuclear Fusion* Vol. 43, No. 9 (September 2003), pp. 822—830, ISSN 0029-5515

Bateman, G. et al (1998) Predicting temperature and density profiles in tokamaks, *Phys. of Plasmas*, Vol.5, No.5 (May 1998), pp. 1793-1799, ISSN 1070-664X

Braginskii, S.I. (1963) Transport processes in a plasma, in *Reviews of Plasma Physics*, edited by Leontovich M., Vol.1, pp.205-310, Library of Congress Catalog Card Number 64-23244, Consultants Bureau, New York, US

Cennachi, G. & Taroni, A. (1988) JETTO: A Free-Boundary Plasma Transport Code (Basic Version), *Rep. JET-IR(88)03*, JET Joint Undertaking, Abingdon, UK

Connor, J.W. & Pogutse, O.P. (2001) On the relationship between mixing length and strong turbulence estimates for transport due to drift turbulence, *Plasma Physics and Controlled Fusion,* Vol.43, No.2, (February 2001), pp. 155-176, ISSN 0741-3335

Diamond, P.H. et al (1994) Self-regulating shear flow turbulence: a paradigm for the L to H transition, *Physical Review Letters,* Vol.72, No.16, (April 1994), pp. 2565-2568, ISSN 0031-9007

Dippel, K.H. et al (1987) Plasma-wall interaction and plasma performance in TEXTOR — A review, *J. Nuclear Mater.* Vol. 145-147, No.2 (February 1987), pp. 3-14, ISSN 0022-3115

Galeev, A.A., and Sagdeev, R.Z., (1973) Theory of neoclassical diffusion, in *Reviews of Plasma Physics*, edited by Leontovich M., Vol.7, pp.257-343, ISBN 0-306-17067-1, Consultants Bureau, New York, US

Gradshteyn, I.S. & Ryzhik, I.M. (1965) Table of integrals, series and products, Academic Press, Library of congress catalog card number 65-29097, New York, US

Greenwald, M. (2002) Density limits in toroidal plasmas. *Plasma Physics and Controlled Fusion,* Vol.44, No.8, (August 2002), pp. R27-R80, ISSN 0741-3335

Guzdar, P.N. et al (2001) Zonal flow and zonal magnetic field generation by finite ß drift waves: a theory for low to high transitions in tokamaks, *Physical Review Letters,* Vol.87, No.1, (July 2001), pp. 015001-1-4, ISSN 0031-9007

Guzdar, P.N. et al. (1993) Three-dimensional fluid simulations of the nonlinear drift-resistive ballooning modes in tokamak edge plasmas, *Phys. Fluids B*, Vol.5, No. 10, (October 1997), pp. 3712-3727, ISSN 0899-8221

Horton Jr., W. et al (1981) Toroidal drift modes driven by ion pressure gradient, *Phys. Fluids*, Vol. 24, No. 6, (June 1981), pp. 1077-1085, ISSN 0031-9171

ITM (2010) http://www.efda-itm.eu/

Jardin, S. (2010) Computational Methods in Plasma Physics, Chapman and Hall/CRC, ISBN 978-1-4398-1021-7, Boca Raton, US

Jardin, S.C. et al (2008) On 1D diffusion problems with a gradient-dependent diffusion coefficient, *J. Comp. Phys.* Vol. 227, No.20, (October 2008), pp. 8769-8775, ISSN 0021-9991

Kadomtsev, B.B. and Pogutse, O.P. (1971) Trapped particles in toroidal magnetic systems, *Nuclear Fusion*, Vol. 11, No. 1, (January 1971), pp. 67-92, ISSN 0029-5515

Kalupin, D. et al, Predictive modelling of L and H confinement modes and edge pedestal characteristics, *Nuclear Fusion* Vol. 45, No. 6 (June 2005), pp. 468–476, ISSN 0029-5515

Kerner, W. (1998) The scaling of the edge temperature in tokamaks based on the Alfven drift-wave turbulence, *Contributions to Plasma Physics*, Vol.38, No.1-2, (January 1998), pp.118-123, ISSN 0863-1042

Lazarus, E.A. et al (1984) Confinement improvement in beam heated ISX-B discharges with low-*z* impurity injection, *J. Nuclear Mater.* Vol. 121, No.1 (May 1984), pp. 61-68, ISSN 0022-3115

Litaudon, X. et al (2007) Development of steady-state scenarios compatible with ITER-like wall conditions, *Plasma Physics and Controlled Fusion,* Vol.49, No.12B, (December 2007), pp. B529-B550, ISSN 0741-3335

Nedospasov, A.V. & Tokar, M.Z. (1993) Plasma edge in tokamaks, in *Reviews of Plasma Physics,* edited by Kadomtsev, B.B., Vol.18, pp.68-20, ISBN 0-306-11007-5, Consultants Bureau, New York, US

Ongena, J. et al (2001) Recent progress toward high performance above the Greenwald density limit in impurity seeded discharges in limiter and divertor tokamaks, *Phys. Plasmas* Vol. 8, No.5 (May 2001), pp. 1364513-1-13, ISSN 1070-664X

Pereverzev, G.V. & Yushmanov, P.N. (1988) Automated System for Transport Analysis in a Tokamak, *IPP Report 5/98*, Max-Planck-Institut für Plasmaphysik, Garching, Germany

Rogers, B.N. et al (1998) Phase space of tokamak edge turbulence, the L-H- transition, and formation of the edge pedestal, *Physical Review Letters,* Vol.81, No.20, (November 1998), pp. 4396-4399, ISSN 0031-9007

Scott, B. (1997) Three-dimensional computation of collisional drift wave turbulence and transport in tokamak geometry, *Plasma Physics and Controlled Fusion,* Vol.39, No.3, (March 1993), pp. 471-504, ISSN 0741-3335

Shestakov, A.I. et al (2003) Self-consistent modelling of turbulence and transport, *J. Comp. Phys.*, Vol.185, No. 2 (March 2003), pp. 399-426, ISSN 0021-9991

Tajima, T. (2004) Computational plasma physics, Westview Press, Boulder, US

Terry, P.W. (2000) Suppression of turbulence and transport by sheared flow, *Rev. Mod. Phys.*, Vol.72, No.1, (January 2000), pp. 109-165, ISSN 0034-6861

Tokar, M.Z. (1993) The possible nature of the localized recycling effect on the plasma edge in tokamaks, *Plasma Physics and Controlled Fusion,* Vol.35, No.9, (September 2007), 1119-1135, ISSN 0741-3335

Tokar, M.Z. (1994) Effect of radial particle transport on radiation from light impurities, *Nuclear Fusion* Vol. 34, No. 6 (June 1994), pp. 853–861, ISSN 0029-5515

Tokar, M.Z. (1994) Modelling of detachment in a limiter tokamak as a nonlinear phenomenon caused by impurity radiation, *Plasma Phys. and Contr. Fusion* Vol. 36, No 11 (November 1994), pp. 1819-1844, ISSN 0741-3335

Tokar, M.Z. (2000a) Model for the transition to the radiation improved mode in a tokamak, *Physical Review Letters,* Vol.84, No.5, (January 2000), pp. 895-898, ISSN 0031-9007

Tokar, M.Z. (2000b) On threshold of radial detachment in tokamaks, *Phys. Plasmas* Vol. 7, No.6 (June 2000), pp. 2432-2438, ISSN 1070-664X

Tokar, M.Z. (2003) Synergy of anomalous transport and radiation in the density limit, *Physical Review Letters,* Vol.91, No.9, (August 2001), pp. 095001-1-4, ISSN 0031-9007

Tokar, M.Z. (2006) Numerical solution of continuity equation with a flux non-linearly depending on the density gradient, *J. Comp. Phys.* Vol. 220, No.1, (December 2006), pp. 2625-2633, ISSN 0021-9991

Tokar, M.Z. (2010) Numerical modeling of transport barrier formation, *J. Comp. Phys.* Vol. 229, No.7, (April 2010), pp. 2625-2633, ISSN 0021-9991

Tokar, M.Z. et al. (2006) Numerical solution of transport equations for plasmas with transport barrier, *Comp. Phys. Comm.* Vol. 175, No.1, (January 2006), pp. 30-35, ISSN 0010-4655

Versteeg, H.K. & Malalasekera, W. (1995) An introduction to computational fluid dynamics: The finite volume method, Harlow: Longman Scientific \& Technical, US

Wagner, F. et al. (1982) Regime of Improved Confinement and High Beta in Neutral-Beam-Heated Divertor Discharges of the ASDEX Tokamak, *Physical Review Letters,* Vol.49, No.19, (November 1982), pp. 1408-1412, ISSN 0031-9007

Waltz, R.E. et al (1197) A gyro-Landau-fluid transport model, *Phys. of Plasmas*, Vol.4, No.7 (July 1997), pp. 2482-2496, ISSN 1070-664X

Weiland, J. (2000) Collective Modes in Inhomogeneous Plasma, Institute of Physics Publishing, ISBN 0-7503-0589-4-hbk, Bristol, Great Britain

Wesson, J. (2004) *Tokamaks, 3rd edition*, Oxford Science Publications, ISBN 0-19-8509227, Oxford, GB

Xu, X.Q et al (2003) , Transitions of turbulence in plasma density limits, *Phys. Plasmas* Vol. 10, No.5 (May 2003), pp. 1773-1781, ISSN 1070-664X

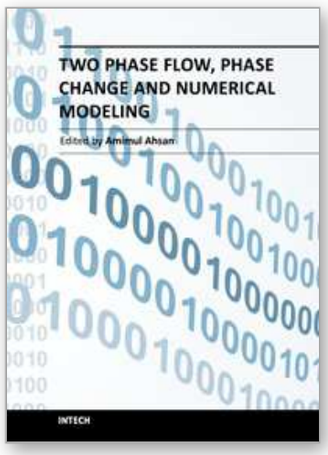

Two Phase Flow, Phase Change and Numerical Modeling

Edited by Dr. Amimul Ahsan

ISBN 978-953-307-584-6
Hard cover, 584 pages
Publisher InTech
Published online 26, September, 2011
Published in print edition September, 2011

The heat transfer and analysis on laser beam, evaporator coils, shell-and-tube condenser, two phase flow, nanofluids, complex fluids, and on phase change are significant issues in a design of wide range of industrial processes and devices. This book includes 25 advanced and revised contributions, and it covers mainly (1) numerical modeling of heat transfer, (2) two phase flow, (3) nanofluids, and (4) phase change. The first section introduces numerical modeling of heat transfer on particles in binary gas-solid fluidization bed, solidification phenomena, thermal approaches to laser damage, and temperature and velocity distribution. The second section covers density wave instability phenomena, gas and spray-water quenching, spray cooling, wettability effect, liquid film thickness, and thermosyphon loop. The third section includes nanofluids for heat transfer, nanofluids in minichannels, potential and engineering strategies on nanofluids, and heat transfer at nanoscale. The forth section presents time-dependent melting and deformation processes of phase change material (PCM), thermal energy storage tanks using PCM, phase change in deep CO2 injector, and thermal storage device of solar hot water system. The advanced idea and information described here will be fruitful for the readers to find a sustainable solution in an industrialized society.

How to reference

In order to correctly reference this scholarly work, feel free to copy and paste the following:

Mikhail Tokar (2011). Modelling of Profile Evolution by Transport Transitions in Fusion Plasmas, Two Phase Flow, Phase Change and Numerical Modeling, Dr. Amimul Ahsan (Ed.), ISBN: 978-953-307-584-6, InTech, Available from: http://www.intechopen.com/books/two-phase-flow-phase-change-and-numerical-modeling/modelling-of-profile-evolution-by-transport-transitions-in-fusion-plasmas

INTECH
open science | open minds

InTech Europe
University Campus STeP Ri
Slavka Krautzeka 83/A
51000 Rijeka, Croatia
Phone: +385 (51) 770 447
Fax: +385 (51) 686 166
www.intechopen.com

InTech China
Unit 405, Office Block, Hotel Equatorial Shanghai
No.65, Yan An Road (West), Shanghai, 200040, China
中国上海市延安西路65号上海国际贵都大饭店办公楼405单元
Phone: +86-21-62489820
Fax: +86-21-62489821

IntechOpen